

Genome-wide identification and analysis of cystatin family genes in Sorghum (*Sorghum bicolor* L.)

Jie Li ^{Corresp. 1}, Xinhao Liu ², Jingmei Wang ², Junyan Sun ¹, Dexian He ^{Corresp. 3}

¹ College of Agronomy, Xinyang Agriculture and Forestry University, Xinyang, Henan Province, China

² Central Laboratory, Xinyang Agriculture and Forestry University, Xinyang, Henan Province, China

³ Collaborative Innovation Center of Henan Grain Crops/National Key Laboratory of Wheat and Maize Crop Science, College of Agronomy, Henan Agricultural University, Zhengzhou, China

Corresponding Authors: Jie Li, Dexian He

Email address: ljxlxh123@126.com, hedexian@126.com

To set a systematic study of the Sorghum *cystatins* (*SbCys*) gene family, a comprehensive genome-wide analysis of the *SbCys* family genes was performed by bioinformatics-based methods. In total, 18 *SbCys* genes were identified in Sorghum, which distributed unevenly on chromosomes, and two genes were involved in tandem duplication event. All *SbCys* genes had similar exon/intron structure and motifs, indicating their high evolutionary conservation. Transcriptome analysis showed that 16 *SbCys* genes were expressed in at least one tested tissues, and most genes displayed higher expression levels in reproductive tissues than in vegetable tissues, indicating that the *SbCys* genes participated in the regulation of seed formation. Furthermore, the expressions of 7 *SbCys* genes were induced by *Bipolaris sorghicola* infection, while only 2 genes were responsive to aphid infestation. In addition, quantitative real-time polymerase chain reaction (qRT-PCR) confirmed that 17 *SbCys* genes were induced by one or two abiotic stresses (dehydration, salt shock and ABA stresses). In addition, the interaction network indicated that *SbCys* proteins were associated with several biological processes, including seed development and stress responses. Notably, the expression of *SbCys4* was up-regulated under biotic and abiotic stresses, suggesting its potential roles in mediating the response of Sorghum to adverse environmental impact. Our results provide new insights into the structural and functional characteristics of *SbCys* gene family, which laid the foundation for better understanding the roles and regulatory mechanism of Sorghum cystatins in seed development and responses to different stress conditions.

1 Genome-wide identification and analysis of cystatin family genes
2 in Sorghum (*Sorghum bicolor* L.)

3 Jie Li¹, Xinhao Liu², Jingmei Wang², Junyan Sun¹, Dexian He^{3*}

4

5 **Author affiliation:**

6 1 College of Agronomy, Xinyang Agriculture and Forestry University, Xinyang, Henan 464001,
7 China

8 2 Central Laboratory, Xinyang Agriculture and Forestry University, Xinyang, Henan 464001,
9 China

10 3 Collaborative Innovation Center of Henan Grain Crops/National Key Laboratory of Wheat and
11 Maize Crop Science, College of Agronomy, Henan Agricultural University, Zhengzhou, Henan,
12 450002, China

13

14 *Corresponding author: Dexian He

15 College of Agronomy, Henan Agricultural University, Zhengzhou, Henan, 450002, China

16 E-mail: hedexian@126.com

17

18

19

20

21

22

23

24 **ABSTRACT**

25 To set a systematic study of the Sorghum *cystatins* (*SbCys*) gene family, a comprehensive
26 genome-wide analysis of the *SbCys* family genes was performed by bioinformatics-based
27 methods. In total, 18 *SbCys* genes were identified in Sorghum, which distributed unevenly on
28 chromosomes, and two genes were involved in tandem duplication event. All *SbCys* genes had
29 similar exon/intron structure and motifs, indicating their high evolutionary conservation.
30 Transcriptome analysis showed that 16 *SbCys* genes were expressed in at least one tested tissues,
31 and most genes displayed higher expression levels in reproductive tissues than in vegetable
32 tissues, indicating that the *SbCys* genes participated in the regulation of seed formation.
33 Furthermore, the expressions of 7 *SbCys* genes were induced by *Bipolaris sorghicola* infection,
34 while only 2 genes were responsive to aphid infestation. In addition, quantitative real-time
35 polymerase chain reaction (qRT-PCR) confirmed that 17 *SbCys* genes were induced by one or
36 two abiotic stresses (dehydration, salt shock and ABA stresses). In addition, the interaction
37 network indicated that *SbCys* proteins were associated with several biological processes,
38 including seed development and stress responses. Notably, the expression of *SbCys4* was up-
39 regulated under biotic and abiotic stresses, suggesting its potential roles in mediating the
40 response of Sorghum to adverse environmental impact. Our results provide new insights into the
41 structural and functional characteristics of *SbCys* gene family, which laid the foundation for
42 better understanding the roles and regulatory mechanism of Sorghum cystatins in seed
43 development and responses to different stress conditions.

44

45

46

47 **INTRODUCTION**

48 Cystatins are competitive and reversible inhibitors of cysteins proteases from families C1A and
49 C13, which have been identified in many plant species (Martinez and Diaz, 2008; Zhao et al.
50 2014). Based on their primary sequence homology, three signature motifs include a QxVxG
51 reactive site, a tryptophan residue (W) located downstream of the reactive site, and one or two
52 glycine (G) residues in the flexible N terminus of the protein. These three motifs are important
53 for the cystatin inhibitory mechanism (Jenko et al. 2003; Stubbs et al. 1990). In addition, a
54 consensus sequence ([LVI]-[AGT]-[RKE]-[FY]-[AS]-[VI]-x-[EDQV]-[HYFQ]-N) in cystatins is
55 conformed to a predicted secondary α -helix structure (Margis et al. 1998). Most plant cystatins
56 are small proteins with a molecular mass in the 12- to 16-kD range (Margis et al. 1998). Some
57 plant cystatins contain a C-terminal extension that raises their molecular weights up to 23 kDa,
58 are thought to be involved in the inhibition of cysteine protease activities in the peptidase C13
59 family (Martinez et al. 2007; Martinez and Diaz, 2008).

60 The principal functions of plant cystatins are related to the regulation of endogenous
61 cysproteases during plant growth and development, senescence, and programmed cell death
62 (Belenghi et al. 2010; Díazmendoza et al. 2014; Zhao et al. 2014). Additionally, Plant cystatins
63 have been used as effective molecules against different pests and pathogens (Martinez et al.
64 2016). For example, several publications reported the inhibition of recombinant cystatins on the
65 growth of some pests and fungi (Martinez et al. 2005; Lima et al. 2015). Tomato plants over-
66 expressing the wheat cystatin *TaMDC1* displayed a broad stress resistance for bacterial pathogen,
67 and the defense responses were mediated by methyl jasmonate and salicylic acid (Christova et al.
68 2018). The inhibition of amaranth cystatin on the digestive insect cysteine endopeptidases was

69 observed by Valdés-Rodríguez et al. (2015). Plant cystatins are also involved in the responses to
70 abiotic stresses, such as over-expression of *MpCYS4* in apple delayed natural and stress-induced
71 leaf senescence (Tan et al. 2017). Song et al. (2017) found that the expression of *AtCYS5* was
72 induced by heat stress (HS) and exogenous ABA treatment in germinating seed, furthermore,
73 over expression of *AtCYS5* enhanced HS tolerance in transgenic *Arabidopsis*.

74 To date, plant cystatin family genes had been well described in several plant species such as
75 *Arabidopsis*, rice, soybean, wheat, and *Populus trichocarpa* (Martinez and Diaz, 2008; Wang et
76 al. 2015; Yuan et al. 2016; Dutt et al. 2016). However, a genome-wide study of cystatins family
77 genes in Sorghum (*Sorghum bicolor* L.) has not yet been performed. Sorghum is the world's fifth
78 biggest crop (after rice, wheat, maize, and barley), belonging to a C4 grass that grows in arid and
79 semi-arid regions (Taylor et al. 2010). Its drought tolerance is a consequence of morphological
80 and anatomical characteristics (i.e., thick leaf wax, deep root system) and physiological
81 responses (i.e., stay-green, osmotic adjustment), is considered as a plant model for drought
82 tolerance in genomic research (Sunita et al. 2011). Recently, the completion of the whole
83 genome assembly of Sorghum (*Sorghum bicolor* L.) makes it possible to identify and analyze
84 cystatin family genes in Sorghum (Paterson et al. 2009). In this study, we aimed to perform a
85 genome-wide identification of *SbCys* family genes in Sorghum and analyze their phylogeny,
86 conserved motifs, structure, *cis*-elements, and expression profile in different tissues. We also
87 explored the expression patterns of *SbCys* genes in response to biotic and abiotic stresses. The
88 results may lay a foundation for further functional analyses of cystatin genes.

89

90 **MATERIALS AND METHODS**

91 **Identification of *SbCys* family members in Sorghum genome**

92 The identification of SbCys candidates was conducted according to the methods of Lozano et al.
93 (2015) with some modification. The cystatin sequences of *Arabidopsis*, rice, and barely were
94 downloaded from TAIR (<http://www.Arabidopsis.org>), the Rice Genome Annotation Project
95 (<http://rice.plantbiology.msu.edu/index.shtml>), and Ensembl database (<http://plants.ensembl.org>),
96 respectively. The whole-genome sequence of Sorghum was downloaded from Ensembl database
97 (<http://plants.ensembl.org>). Then predicted proteins from Sorghum genome were scanned using
98 HMMER v3 (<http://hmmer.org/>) using the Hidden Markov Model (HMM) profile of cystatin
99 (PF00031) from Pfam protein family database (<http://pfam.xfam.org/>) (Finn et al. 2011). From
100 the proteins obtained using the raw cystatin HMM, a high-quality protein set with a cut-off *e*-
101 value $< 1 \times 10^{-10}$ was aligned and used to construct a Sorghum specific cystatin HMM using
102 hmmbuild from the HMMER v3 suite. Then all proteins with *e*-value < 0.01 were selected by the
103 new Sorghum specific HMM. Cystatin sequences were further filtered based on the closest
104 homolog from *Arabidopsis*, rice and barely using ClustalW and the UNIREF100 sequence
105 database. Proteins without typical domain (Aspartic acid proteinase inhibitor) and reactive site
106 motif (QxVxG) were removed from posterior analysis.

107 **Sequence alignment, structure analysis, and phylogenetic tree construction**

108 The Multiple Expectation for Motif Elicitation (MEME) program was used to identify conserved
109 motifs shared among SbCys proteins. The parameters of MEME were as follows: maximum
110 number of motifs, 10; optimum width, between 6 and 50; and number of repetitions, any.

111 The three-dimensional structures of Sorghum cystatins were modelled by the automated SWISS-
112 MODEL program (<http://swissmodel.expasy.org/interactive>) (Peitsch 1996). The known crystal
113 structure of rice oryzacystatin I (OC-I) (Nagata et al. 2000) and SiCYS (Hu et al. 2015) were
114 used to construct the homology-based models. Structure analysis was conducted by the RasMol

115 2.7 program (Sayle and Milner-White 1995).

116 A phylogenetic tree was constructed using MEGA X with the maximum likelihood method
117 according to the Whelan and Goldman + freq. Model. Bootstrap analysis was performed by 1000
118 replicates with the p-distance model. The phylogenetic tree was visualized and optimized in
119 Figtree (<http://tree.bio.ed.ac.uk/software/figtree/>).

120 **Transcript structures, chromosomal location and gene duplication**

121 The genomic structure of each *SbCys* gene was derived from the alignment of their coding
122 sequence to their corresponding genome full-length sequence. The diagrams of these *SbCys*
123 genes were drawn by the Gene Structure Display Server (GSDS, <http://gsds.cbi.pku.edu.cn/>)
124 (Hu et al. 2014). The chromosomal locations of *SbCys* genes were retrieved from the
125 *Sorghum_bicolor_NCBIv3* map. The genes were plotted on chromosomes using the Map
126 Gene2chromosome (MG2C, version 2.0) tool (<http://mg2c.iask.in/>). Gene duplication events of
127 *SbCys* family genes were investigated according to the following two criteria: (1) the alignment
128 covered > 75% of the longer gene, (2) the aligned region had an identity > 75%, (3) located in
129 less than 100 kb single region or separated by less than five genes (Gu et al. 2002). For
130 microsynteny analysis, the CDS sequence of every cystatin from *Arabidopsis*, barley, rice, and
131 *Sorghum* was used as the query to search against all other cystatins using NCBI_blast software
132 with $e\text{-value} \leq 1e^{-10}$. The Circos software was used to display the results of collinearity gene
133 pairs (Krzywinski et al. 2009).

134 **Calculation of Ka and Ks**

135 To assess the degree of natural selection on *SbCys* genes, the rate ratio of *Ka* (nonsynonymous
136 substitution rate) to *Ks* (synonymous substitution rate) was calculated using KaKs Calculator 2.0
137 (Zhang et al. 2006). The *Ka/Ks* ratio > 1, < 1, or = 1 indicates positive, negative, or neutral

138 evolution, respectively (Yadav et al. 2015).

139 **Promoter analysis of *SbCys* genes**

140 To investigate the *cis*-regulatory elements in a promoter region, the upstream sequences (1.5 kb)
141 of the start codon in each *SbCys* gene were scanned in the PlantCARE database
142 (<http://bioinformatics.psb.ugent.be/webtools/plantcare/html/>) and New PLACE
143 (<https://www.dna.affrc.go.jp/PLACE/?action=newplace>).

144 **Analysis of interaction networks of the *SbCys* proteins**

145 The functional interacting network models of *SbCys* proteins were integrated using the web
146 STRING program (<http://string-db.org/>) based on an *Arabidopsis* association model; the
147 confidence parameters were set at a 0.40 threshold, the number of interactors was set to five
148 interactors. *Arabidopsis* AtCys proteins were mapped to Sorghum *SbCys* proteins based on their
149 homologous relationship, and the interaction network of *SbCys* proteins was drawn by
150 Cytoscape_v3.6.0.

151 **Expression analysis of *SbCys* genes under biotic stresses**

152 The RNA-Seq data used for investigating the expression patterns of *SbCys* genes in various
153 tissues were downloaded from NCBI SRA (Sequence Read Archive) database (ERP024508)
154 (Wang et al. 2018). Root, shoot, and whole organism were collected at 14 days after germination.
155 Embryo, endosperm and pericarp were collected at 20 days after pollination. Pollen samples
156 were collected at booting stage. Inflorescences were collected according to the sizes: 1-5 mm, 5-
157 10 mm, and 1-2 cm. Three biological replicates were performed for each plant tissue. RNA was
158 sequenced using the Illumina HiSeq 2500 system to generate 250 bp pair-end reads.
159 RNA-seq data of biotic stresses were obtained from two experiments. The first experiment
160 measured the transcriptome response of a resistant Sorghum (*Sorghum bicolor* L. Moench)

161 infected with *Bipolaris sorghicola* (DRP 000986) (Yazawa et al. 2013). RNA samples were
162 collected at 0, 12 and 24 hours post-inoculation with one biological replicate. RNA-seq was run
163 using Illumina technology to give 100-base-pair single-end reads on a HiSeq2000 system. The
164 second study measured changes in the transcriptome of Sorghum leaves infested by sugarcane
165 aphid (Tetreault et al. 2019). The RNA-seq data were downloaded from the NCBI SRA database
166 (SRP162227). In this study, two treatments (infested and control) were arranged and two
167 Sorghum genotypes (resistant cultivar RTx2783 and susceptible cultivar BCK60) were used.
168 Leaf samples were collected from treated and control plants at 5, 10 and 15 days post sugarcane
169 aphid infestation. Three biological replicates were performed for all treatment and time
170 combinations. RNA was sequenced using the Illumina Hiseq 2500 platform to generate 100 bp
171 single end reads. The accession numbers and sample information were listed in Table S1. The
172 differential expression of *SbCys* genes were investigated by Hisat2 (<http://kim-lab.org/>), Htseq
173 (<http://www.htseq.org/>), and DESeq2 (R package) based on the RNA-seq data (Wen, 2017). The
174 $p \leq 0.05$ and $|\logFC| \geq 1.5$ were set as the cut-off criterion.

175 **Plant materials and treatments**

176 Seed of Sorghum (*Sorghum bicolor* L. cv. Jinza 35) were surface sterilized (15 min in 4%
177 NaClO), washed with distilled water several times, and transferred to moist germination paper
178 for 3 days in an incubator at 25 °C. These seedlings were grown in holes of foam floating plastic
179 containers (30 seedlings per container) with constant aeration in Hoagland solution in a growth
180 room with 14 h/30 °C light and 10 h/22 °C dark regime. The nutrient solution was routinely
181 changed every 3 days. At the three-leaf stage (the juvenile phase (Hashimoto et al. 2019)),
182 abiotic stresses including ABA, salinity, and dehydration treatments were initiated according to
183 the procedures described in previous reports (Dugas et al. 2011; Wang et al. 2012; Yan et al.

184 2017). The plants were transferred quickly to the nutrient solution containing 0.1 mM ABA
185 (dissolved in ethanol), 5 μ L ethanol (control for ABA treatment), 250 mM sodium chloride
186 (NaCl), or 15% (W/V) polyethylene glycol (PEG) 6,000. The central part of flag leaves from
187 randomly selected Sorghum plants were harvested respectively at 0, 12 and 24 hours post-
188 treatment per trial, and immediately frozen in liquid nitrogen and stored at -80 °C prior to RNA
189 isolation. For each treatment at a given time, three biological replicates were used. The leaf
190 samples of 10 plants came from the same container for one biological replicate. That is, three
191 containers were used for three biological replicates respectively.

192 **RNA extraction and qRT-PCR analysis**

193 Total RNA of 100 mg leaf samples was isolated using the “TaKaRa MiniBEST Plant RNA
194 Extraction” Kit (TaKaRa, Dalian, China) following the manufacturer’s instructions. Purity and
195 concentration of RNA samples were evaluated by measuring the A_{260}/A_{230} and A_{260}/A_{280} ratios.
196 In order to digest the genomic DNA, the RNAs were treated with RNase-free DNase I. Reverse
197 transcription was performed according to the kit instruction (Promega, Madison, USA). Primer
198 pairs for qRT-PCR analysis were designed by Primer3Plus program
199 (<http://www.bioinformatics.nl>), and shown in Table S2. A 20 μ l reaction volume containing 0.4
200 μ l of each primer (forward and reverse), 2 μ l 10-fold diluted cDNA, 7.2 μ l of nuclease-free water
201 and 10 μ l of GoTaq® qPCR Master Mix (Perfect Real Time; Promega). PCR reaction included
202 one cycle at 95 °C for 3 min, followed by 39 cycles of 95 °C for 15 s, 60 °C for 30s and 72 °C for
203 20s. The reactions were conducted using CFX96 Real-Time PCR Detection System (Bio-Rad
204 Laboratories, Inc.). Three independent biological replicates and two technical replicates of each
205 sample were performed. Gene-specific amplification of both reference and *cystatin* genes were
206 standardized by the presence of a single, dominant peak in the qRT-PCR dissociation curve

207 analyses. All data were analyzed by CFX Manager Software (Bio-Rad Laboratories, Inc.). The
208 efficiency range of the qRT-PCR amplifications for all of the genes tested was between 91% and
209 100%. The average target (*SbCys*) cT (threshold cycle) values were normalized to reference (β -
210 *actin*) cT values. The fold change between treated sample and control was calculated using the
211 slightly modified $2^{-(\Delta\Delta C_t)}$ method as described by Kebrom et al. (2010). A probability of $p \leq 0.05$
212 was considered to be significant.

213

214 RESULTS

215 Identification and analysis of *SbCys* genes

216 To extensively identify all of *SbCys* family members in Sorghum, we constructed a Sorghum-
217 specific HMM for the *SbCys* domain to scan Sorghum genome, and 22 gene candidates were
218 identified. After removing the repetitive and/or incomplete sequences, the rest of *SbCys*
219 sequences were submitted to Pfam (<http://pfam.xfam.org/>) and SMART ([http://smart.embl-
220 heidelberg.de/](http://smart.embl-heidelberg.de/)) to confirm the conserved domain. Finally, a total of 18 non-redundant *SbCys*
221 proteins were identified and were serially renamed from *SbCys1* to *SbCys17* according to their
222 location and order in chromosomes. Gene names, gene IDs, chromosomal locations, amino acid
223 numbers and protein sequences were listed in Table S3. The average length of these *SbCys*
224 proteins was 148 amino acid residues and the length mainly centered on the range of 105 to 240
225 amino acid residues.

226 Chromosome distribution analysis showed that the number of *SbCys* genes on each chromosome
227 is different (Fig. 1). Chromosome 1 had the greatest number of *SbCys* genes (9 genes), followed
228 by chromosomes 9 and 3 (4 and 3 genes, respectively). Chromosomes 2 and 4 had just one
229 *SbCys* gene, whereas chromosomes 5, 6, 7, 8 and 10 had no *SbCys* genes. Half of *SbCys* genes

230 were distributed on chromosome 1, suggesting that *SbCys* genes may have a chromosomal
231 preference.

232 **Gene structure analysis of *SbCys* genes**

233 The analysis of exon-intron structure can provide significant information about the gene function,
234 organization and evolution of multiple gene families (Xu et al. 2012). Schematic structures of
235 *SbCys* genes from Sorghum were obtained using the GSDS program (Fig. 2). Among the *SbCys*
236 genes, more than half (12, 66.7%) were intronless, three genes (*SbCys11*, *SbCys15*, and *SbCys16*)
237 had one intron, two genes (*SbCys14* and *SbCys17*) had two introns, and one gene (*SbCys10*) had
238 three introns. These six *SbCys* genes with one or more introns were clustered into one clade,
239 suggesting the evolutionary event may effect on the gene structure (Altenhoff et al. 2012).

240 **Sequence alignment, protein motifs analysis, and structural predication of SbCys**

241 Alignments of SbCys sequences were carried out to search for amino acid variants that could
242 lead to differences in their inhibitory capability for cysteine proteases. The results were shown in
243 Fig. 3a. N-terminal and C-terminal extensions with varying lengths that presented in several
244 SbCys proteins were not displayed in the comparison. These predicted structures shared many
245 identical residues including α -helix and the four β -sheets (β 2-5) (Fig. 3a). Analysis of conserved
246 motifs of SbCys proteins also revealed that some typical conserved motifs could be detected in
247 most SbCys proteins, such as motif 1, 2, 3, and 4, form a fundamental structural combination
248 (Fig. 3b and 3c). Motif 1 was conserved in the central loop region with a consensus sequence of
249 “QxVxG” and could be detected in most SbCys proteins, which played an important role in the
250 inhibitory capacity of cystatins towards their target cysteine proteases (Meriem et al. 2010).
251 Motif 2 contained a particular consensus sequence ([LVI][GA][RQG][WF]AV) that conformed
252 to a predicted secondary α -helix structure (Martinez et al. 2009). The other two typical motifs for

253 SbCys proteins, motif 3 (V[WY][EVG]KPW) and motif 4 ([RK]xLxxF), were firstly described
254 in tobacco (Zhao et al. 2014), were also detected in most SbCys proteins, indicating their
255 conserved and common role in both dicots and monocots. Motif 5 existed only in 3 SbCys family
256 members (SbCys5, SbCys8, and SbCys15,). Details of the 5 conserved motifs were shown in Fig.
257 S1.

258 The predicted three-dimensional structures of the Sorghum cystatins were established using the
259 SWISS-MODEL program based on the known crystal structure of OC-I and SiCYS (Fig. 4).
260 Although these structures were predicted with variable degrees of accuracy, all of Sorghum
261 cystatins shared similar protein structure with rice OC-I (Fig. 4a), excepting SbCys10 that shared
262 similar protein structure with SiCYS (Fig. 4b). In addition, SbCys14 showed a significant
263 variation in its predicted three-dimensional structures, an extra α -helix occurred in the C-terminal
264 region, which probably due to the cystatin contained a C-terminal extension. Two important
265 motifs (the conserve QxVxG motif and W residue) of Sorghum cystatins involved in the
266 interaction with the target cysteine enzymes were also shown in Fig. 4. The predicted structure of
267 SbCys13 showed some distortions in the region of the β 2 sheet, probably due to the insertion of a
268 methionine in the first position of the conserved QxVxG motif.

269 **Phylogenetic analysis of *SbCys* genes**

270 Cystatin gene family is highly conserved in both monocots and dicotyledons (Martinez and Diaz,
271 2008). To investigate the phylogenic relationships of SbCys proteins to other known plant
272 cystatins, a multiple sequence alignment of SbCys sequences to the sequences from *Arabidopsis*,
273 rice, and barley was conducted by the ClustalW program. As showed in Fig. 5, these cystatins
274 were categorized into three groups, including Group I, Group II, and Group III. A total of 21
275 cystatins were classified to Group I and 6 cystatins from Sorghum. Group II contained 7

276 cystatins, only one cystatin from Sorghum. The remaining 21 proteins were assigned to Group III
277 and 11 *SbCys* proteins fell into this group. In addition, some bootstrap values in the phylogenetic
278 tree were low, suggesting that high sequence differentiation in these cystatins occurred.
279 Microsynteny analysis indicated that one orthologous gene pair was identified in the cross of
280 barley and Sorghum, rice and Sorghum, respectively, while no orthologous gene pair between
281 *Arabidopsis* and Sorghum was found (Fig. S2). These data indicated that *SbCys* genes were more
282 closely to those of rice and barley than that of *Arabidopsis*. Interestingly, a pair of *SbCys* genes
283 (*SbCys2-1* and *SbCys2-2*) was confirmed to be tandem duplication in Sorghum (Fig. S2).
284 Analysis of duplicated *SbCys* genes showed that the *Ka/Ks* ratios far less than 1, varying from
285 0.0976 to 0.5679 (Table S4), indicating that negative selection occurred in the duplication event.

286 **Promoter analysis of *SbCys* genes**

287 In order to obtain useful information on the regulatory mechanism of cystatin gene expression,
288 the 1.5 kb upstream sequences from the translation start sites of *SbCys* genes were submitted into
289 PlantCARE database to detect the *cis*-elements. Various putative plant regulatory elements in the
290 promoter region of *SbCys* genes were shown in Fig. 6 and Table S5. Several potential regulatory
291 elements involved in stress-related transcription factor-binding sites were found, including G-
292 box, W-box, TC-rich repeats, MBS, heat shock elements (HSEs), and ABA-response element
293 (ABRE). The identified *SbCys* genes possessed at least 1 stress-response-related *cis*-element,
294 suggesting that the expressions of *SbCys* genes were related to these abiotic stresses. All of
295 *SbCys* genes had one or more G-box with the exception of *SbCys9*, implying that these *SbCys*
296 genes could be induced by light stress. 14 *SbCys* genes possessed MBS element, ABRE element
297 was found in 12 *SbCys* genes, and HSE element was located in 10 *SbCys* genes. TC-rich repeats
298 and W-boxes were located in 8 genes, respectively. In addition, Skn-1_motif was conserved in

299 the promoter regions of most *SbCys* genes, indicating these genes were associated with the
300 regulation of seed storage protein gene expression (Strömviik and Fauteux, 2009). The high
301 diversity of the *cis*-acting elements suggested that these *SbCys* genes might have a wide range of
302 functional roles and could be involved in multiple stress responses and growth and development
303 progress (Zhang et al. 2008).

304 **Protein interaction network of SbCys proteins**

305 In this study, the interactions of the *SbCys* proteins were investigated in an *Arabidopsis*
306 association model using STRING software. As shown in Fig. 7, the interaction network of
307 cystatins showed a complex functional relationship. *AtCys2* (corresponding to *SbCys12*)
308 interacted with stress related proteins (*AT1G56280*, *AT3G19580*, *AT5G67450*, and *AtCys1*) and
309 growth and development related proteins (*AT1G63100* and *AT5G04340*), *AtCys1*
310 (corresponding to *SbCys11*, 15, 16, and 17) interacted with some vacuolar-processing enzyme
311 which involved in processing of vacuolar seed protein precursors into the mature forms, and
312 *AtCys5* (corresponding to *SbCys1*, 2-1, 3, 4, 5, 6, 7, 8, 9, and 13) interacted with several lipid-
313 transfer proteins (*AT1G07747*, *AT1G52415*, *AT2G16592*, *AT3G29152*, and *AT4G12825*). The
314 results suggested that cystatins might be associated with many biological processes by protein
315 interactions, such as pollen development, stress responses, and seed maturation (Wang et al.
316 2012).

317 **Expression profile of SbCys genes in different Sorghum tissues**

318 To obtain the spatial and temporal expression patterns of all *SbCys* genes, RNA-seq data
319 (ERP024508) were downloaded to explore the expression levels of *SbCys* genes in different
320 tissues including root, stem, whole organism, pollen, endosperm, embryo, inflorescence (1-5mm,
321 1-10mm, and 1-2cm), and pericarp. As shown in Fig. 8 and S3, most *SbCys* genes were

322 expressed in one tissue at least, except for *SbCys13*, which were barely expressed in any tissue.
323 The expression patterns of *SbCys* genes in reproductive tissues were significantly difference
324 from vegetable tissues. Such as *SbCys2-1*, *SbCys3*, *SbCys4*, *SbCys5*, *SbCys7*, *SbCys9*, *SbCys12*,
325 and *SbCys17* showed relatively higher expression levels in reproductive tissues including pollen,
326 endosperm, embryo, and pericarp than in vegetable tissues, while the expression of *SbCys7* and
327 *SbCys15* were higher in vegetable tissues than in reproductive tissues. It was worth noting that
328 majority of *SbCys* genes had lower expression levels during inflorescence development
329 excepting for *SbCys17* which displayed higher expression pattern.

330 **Expression of *SbCys* genes under biotic stresses**

331 To gain insight into the potential roles of *SbCys* genes in response to *Bipolaris sorghicola*
332 infection and sugarcane aphid infestation, their relative expression patterns were investigated by
333 using the public transcription data from NCBI SRA database (DRP000986 and SRP162227,
334 respectively). As shown in Fig. 9 and 10, the expression patterns of *SbCys* genes were different
335 under the two biotic stresses. In response to *Bipolaris sorghicola* infection, seven *SbCys* genes
336 were induced and only 2 genes (*SbCys12* and *SbCys13*) were suppressed in infected Sorghum
337 leaves compared with control (Fig. 9a). However, under aphid infestation, four *SbCys* genes
338 (*SbCys4*, *SbCys10*, *SbCys11*, and *SbCys14*) were up-regulated and 3 genes (*SbCys1*, *SbCys3*, and
339 *SbCys17*) were down-regulated relative to control in susceptible Sorghum line (BCK60). In
340 resistant Sorghum line (RTx2783), only two *SbCys* genes (*SbCys4* and *SbCys11*) were induced,
341 and the rest were barely expressed in Sorghum leaves with aphid infection (Fig. 9b and 10).
342 These results might suggest that *SbCys* genes played different roles in responding to pathogen
343 infection and aphid infestation.

344 **Expression profiling of *SbCys* genes under abiotic stresses**

345 We also investigated the expression of *SbCys* genes in response to various abiotic stresses
346 including dehydration, salt shock, and ABA (Fig. 11). Under dehydration stress, seven *SbCys*
347 genes (*SbCys4*, *SbCys5*, *SbCys6*, *SbCys9*, *SbCys10*, *SbCys11*, and *SbCys17*) were induced to
348 present a significant up-regulation from 0 to 24 h, while the expressions of *SbCys2-1*, *SbCys12*,
349 *SbCys15*, and *SbCys16* were decreased. Furthermore, the expressions of 4 *SbCys* genes (*SbCys1*,
350 *SbCys3*, *SbCys8*, and *SbCys14*) displayed an up-down trend from 0 h to 24 h (Fig. 11a). With salt
351 shock treatment, the expressions of *SbCys2-1*, *SbCys3*, *SbCys4*, *SbCys8*, *SbCys10*, and *SbCys11*
352 were significantly up-regulated at all treatment time points, whereas *SbCys16* showed a
353 significant down-regulated trend (Fig. 11b). In addition, *SbCys6*, *SbCys13*, *SbCys14*, *SbCys15*,
354 and *SbCys17* showed up and down expression trends, but *SbCys5* displayed down and up
355 expression pattern (Fig. 11b). After exogenous ABA treatment, the expressions of 4 *SbCys* genes
356 (*SbCys2-2*, *SbCys3*, *SbCys4*, and *SbCys7*) were significantly up-regulated at all time points, but 9
357 genes (*SbCys1*, *SbCys2-1*, *SbCys5*, *SbCys8*, *SbCys10*, *SbCys11*, *SbCys13*, *SbCys14*, and *SbCys17*)
358 were down-regulated. Additionally, *SbCys12*, *SbCys15*, and *SbCys16* displayed an up-down
359 expression trends (Fig. 11c). Interestingly, all *SbCys* genes were up-regulated in response to one
360 or two stresses except *SbCys4* that was significantly induced under dehydration, salt shock and
361 ABA stresses, suggesting that *SbCys4* might play an important role in response to different stress
362 responses.

363

364 **DISCUSSION**

365 Plant cystatins are a group of intrinsic small proteins, whose members play important roles in
366 diverse biological processes and stress responses (Martinez et al. 2016; Meriem et al. 2010).
367 Recently, a large number of sequence data from different plant species have been uploaded in

368 GenBank, which provide convenience for us to describe their characteristics, and several
369 cystatins families have been identified from plants, such as rice, soybean and wheat (Wang et al.
370 2015; Dutt et al. 2016; Yuan et al. 2016). However, little is known about cystatin family in
371 Sorghum. In the present study, we identified 18 *SbCys* genes from Sorghum genome. The
372 number was less than that of *B. distachyon* genome, where 25 *BdCys* members were identified
373 (Subburaj et al. 2017). The 18 members in Sorghum was a larger number than found in rice (11
374 genes) and *Arabidopsis* (7 genes) (Wang et al. 2015), but was similar to soybean (20 members)
375 (Yuan et al. 2016). The difference on the cystatin number might reflect the adaptation of plants
376 to environment.

377 The identified *SbCys* genes were unevenly distributed on chromosomes 1, 2, 3, 4, and 9, and half
378 of them were distributed on chromosome 1 (Fig. 1), suggesting that *SbCys* genes had a
379 chromosomal preference. The uneven distribution of *cystatin* genes in chromosomes was also
380 found in *B. distachyon* genome that the highest number of *BdCys* genes located in chromosome 1
381 (Subburaj et al. 2017). The phenomenon of chromosomal preference was also observed in *Oryza*
382 *sativa* genome, but most *OsCys* genes were dispersed over two chromosomes, chromosome 1
383 and 3 (Wang et al. 2015). Furthermore, several tandem duplication events occurred at
384 chromosomes 1 of *B. distachyon* genome (Subburaj et al. 2017). Two tandem duplication events
385 (*OsCys4/OsCys5* and *OsCys6/OsCys7*) were found among *OsCys* genes, and existed in
386 chromosomes 1 and 3 (Wang et al. 2015). One tandem duplication event (*SbCys2-1/SbCys2-2*)
387 occurred among *SbCys* genes at chromosome 1 (Fig. S2). The tandem duplication events might
388 cause the distinct distribution patterns of *cystatin* genes on the chromosomes (Li et al. 2017).

389 Eighteen *SbCys* genes were divided into three groups based on phylogenetic analysis (Fig. 5).
390 Some conserved motifs among *SbCys* proteins had been identified by the alignment of the amino

391 acid sequences (Fig. 3). However, the conservation was accompanied with differences in some
392 important amino acids, indicating that SbCys family members might undergo a complex
393 evolutionary history, which would have a significant influence on their respective functions
394 (Abraham et al. 2006). For example, QxVxG motif, could directly enter and interact with the
395 active site of targeted enzymes, were conserved in all SbCys proteins with the exceptions of 5
396 cystatins (SbCys1, SbCys6, SbCys8, SbCys9, and SbCys13) that were partially modified by the
397 insertion or variation in important residues (Fig. 3a). Furthermore, three SbCys proteins (SbCys8,
398 SbCys9, and SbCys13) showed significant variations with other Sorghum cystatins in their
399 predicted three-dimensional structures (Fig. 4). The variations in vital amino acid residues might
400 result in the change in cystatin inhibitory action (Melo et al. 2003). In addition, two novel motifs,
401 motif 3 (V[WY][EVG]KPW) and motif 4 ([RK]xLxxF), firstly described in tobacco (Zhao et al.
402 2014), were also identified in the C-terminalin of many SbCys proteins. The contribution of the
403 two new motifs to cystatin inhibitory action needs to be further studied.

404 During past decades, plant cystatins were reported to play essential roles in inhibiting
405 endogenous and exogenous cysteine proteases activities during seed development (Gaddour et al.
406 2001; Kiyosaki et al. 2007). In the present study, as revealed by RNA-seq data analysis (Fig. 8
407 and S3), the expression levels of several *SbCys* family genes were higher in reproductive tissues
408 than in vegetable tissues, which were consistent with the reports that most cystatins were
409 specifically expressed in developing seeds and played a role in seed development (Dutt et al.
410 2010; Zhao et al. 2014). Moreover, promoter analysis showed that the highly expressed *SbCys*
411 genes in reproductive tissues possessed endosperm expression related *cis*-elements (Skn-1 and
412 GCN4_motif) (Fig. 6 and Table S5). Our protein interaction prediction results also showed that
413 several SbCys proteins could interact with many functional proteins (Fig. 7), implying these

414 cystatins were involved in regulating the gene expression of cereal grain storage proteins (Diaz-
415 Mendoza et al. 2016).

416 Plant cystatins are involved in various biotic stress responses and probably act as defense
417 proteins against pests and pathogen infection (Meriem et al. 2010). At present, some cystatins
418 with insecticidal activity have been isolated from barley, corn, tomato and papaya etc. (Alvarez-
419 Alfageme et al. 2007; Goulet et al. 2008; Kiggundu et al. 2010), and several cystatins having
420 antifungal activities were also isolated from taro, cacao, and wheat (Christova et al. 2006;
421 Pirovani et al. 2010; Chen et al. 2014). Although studies on insecticidal and antifungal activity of
422 plant cystatins have been well established in vitro, the knowledge about their roles in plants in
423 response to biotic stresses is limited. To explore the properties of *SbCys* genes responding to pest
424 and pathogen infection, we conducted the analysis on the expression patterns of *SbCys* genes.
425 The results showed that the expressions of most *cystatin* genes were induced during *Bipolaris*
426 *sorghicola* infection, suggesting these cystatins played functions in inhibiting exogenous
427 cysteine proteases secreted by pathogens to infect plant tissues (Fig. 9a). Interestingly, for
428 sugarcane arthropods infestation, only two genes (*SbCys4* and *SbCys11*) were up-regulated
429 significantly in susceptible and resistant Sorghum lines (Fig. 9b and 10), the expressions of the
430 rest genes were no obvious change or were down-regulated. These differential expression
431 patterns between *SbCys* genes might suggest that some of them had evolved to inhibit specific
432 cysteine proteinases. The exact roles of these *SbCys* genes in insecticidal and antifungal activity
433 in vivo are worthy to be explored in the further study.

434 Another characteristic of cystatin genes is that they are involved in various abiotic stress
435 responses in different plant species, such as rice, barley, and maize (Gaddour et al. 2001;
436 Massonneau et al. 2005; Huang et al. 2007). In *Arabidopsis*, the expression levels of *AtCYS1* and

437 *AtCYS2* were enhanced by high temperature and wounding stresses (Hwang et al. 2010). *AtCYSa*
438 and *AtCYSb* were also induced by different abiotic stresses such as salt, drought, oxidation and
439 cold stresses (Zhang et al. 2008). Velasco-Arroyo et al. (2018) reported that the silence of barley
440 *HvCPI-2* and *HvCPI-4* specifically modified leaf responses to drought stress. Wang et al. (2015)
441 observed the significant change in the expression levels of several rice *OsCYS* genes under cold,
442 drought, salt, and hormone treatments. In the present study, most *SbCys* genes were found to
443 have positive or negative responses to dehydration, salt shock, and ABA stresses. Moreover, the
444 interaction results showed that most cystatins could interact with stresses-related proteins,
445 implying that the cystatins played critical roles in response to diverse stress conditions. Notably,
446 the expression of *SbCys4* was significantly up-regulated under three stress conditions (Fig. 11),
447 suggesting a specific role of *SbCys4* in responding to various stress conditions. Promoter
448 analysis indicated that stress-related *cis*-elements were widespread in the promoter region of
449 these cystatin genes (Table S5), and *SbCys4* possessed plenty of stress-related *cis*-elements,
450 including G-box, ABRE, HSE, MBS and TC-rich repeats. These results provide an effective
451 reference for the functional verification of the *SbCys* family genes under abiotic stresses.

452

453 CONCLUSIONS

454 In the current study, we identified 18 *SbCys* family genes in Sorghum genome through a
455 genome-wide survey. The chromosomal localization, conserved protein domain, gene structure,
456 the phylogenetic relationship, as well as the interaction network of these *SbCys* genes was
457 systematically analyzed, revealing special characteristics of *SbCys* family genes in Sorghum. The
458 identified *SbCys* genes displayed an uneven distribution in Sorghum chromosomes. All *SbCys*
459 genes shared similar exon/intron organization and conserved motifs. Phylogenetic analysis

460 suggested that Sorghum cystatins had higher homology with monocotyledon than dicotyledon.
461 The variation of amino acids in Sorghum cystatin critical active sites suggested that they might
462 undergo a complex evolutionary process and possess structural and functional divergence. The
463 expression profile of *SbCys* genes in different tissues indicated that most *SbCys* genes were
464 involved in tissue growth and development. Changes in the expression of *SbCys* genes under
465 biotic and abiotic stresses indicated that many *SbCys* genes played important roles in response to
466 unfavorable growth conditions. It was noting that the expression of *SbCys4* was significantly
467 enhanced under biotic and abiotic stresses, suggesting its unique role in mediating the response
468 of Sorghum to adverse environment conditions.

469

470 REFERENCES

- 471 **Abraham Z, Martinez M, Carbonero P, Diaz I. 2006.** Structural and functional diversity
472 within the cystatin gene family of *Hordeum vulgare*. *Journal of Experimental Botany*
473 **57(15):4245-4255** DOI 10.1093/jxb/erl200.
- 474 **Altenhoff AM, Studer RA, Robinsonrechavi M, Dessimoz C. 2012.** Resolving the ortholog
475 conjecture: orthologs tend to be weakly, but significantly, more similar in function than
476 paralogs. *PLoS Computational Biology* **8(5):e1002514** DOI
477 10.1371/journal.pcbi.1002514.
- 478 **Alvarez-Alfageme F, Martinez M, Pascual-Ruiz S, Castanera P, Diaz I, Ortego F. 2007.**
479 Effects of potato plants expressing a barley cystatin on the predatory bug *Podisus*
480 *maculiventris* via herbivorous prey feeding on the plant. *Transgenic Research* **16:1-13** DOI
481 10.1007/s11248-006-9022-6.
- 482 **Belenghi B, Acconcia F, Trovato M, Perazzolli M, Bocedi A, Polticelli F, Ascenzi P,**

- 483 **Delledonne M. 2010.** AtCYS1, a cystatin from *Arabidopsis thaliana*, suppresses
484 hypersensitive cell death. *European Journal of Biochemistry* **270(12):2593-604** DOI
485 10.1046/j.1432-1033.2003.03630.x.
- 486 **Blanca VA, Mercedes DM, Andrea GS, Santamaria B, Estrella M, Miguel TB, Kumlehn G,**
487 **Martinez J, Diaz I. 2018.** Silencing barley cystatins *HvCPI-2* and *HvCPI-4* specifically
488 modifies leaf responses to drought stress. *Plant Cell Environment* **41:1776-1790** DOI
489 10.1111/pce.13178.
- 490 **Chen PJ, Senthilkumar R, Jane WN, He Y, Tian Z, Yeh KW. 2014.** Transplastomic
491 *Nicotiana benthamiana* plants expressing multiple defence genes encoding protease
492 inhibitors and chitinase display broad-spectrum resistance against insects, pathogens and
493 abiotic stresses. *Plant Biotechnology Journal* **12(4):1-13** DOI 10.1111/pbi.12157.
- 494 **Christova PK, Christov NK, Imai R. 2006.** A cold inducible multidomain cystatin from winter
495 wheat inhibits growth of snow mold fungus, *Microdochium nivale*. *Planta* **223:1207-1218**
496 DOI 10.1007/s00425-005-0169-9.
- 497 **Christova PK, Christov NK, Mladenov PV, Imai R. 2018.** The wheat multidomain cystatin
498 TaMDC1 displays antifungal, antibacterial, and insecticidal activities in planta. *Plant Cell*
499 *Reports* **37:923-932** DOI 10.1007/s00299-018-2279-4.
- 500 **Diaz-Mendoza M, Dominguez-Figueroa JD, Velasco-Arroyo B, Cambra I, Gonzalez-**
501 **Melendi P, Lopez-Gonzalez A, Garcia A, Hensel G, Kumlehn J, Diaz I, Martinez**
502 **M. 2016.** HvPap-1 C1A protease and HvCPI-2 cystatin contribute to barley grain filling
503 and germination. *Plant Physiology* **170:2511-2524.** DOI 10.1104/pp.15.01944.
- 504 **Díazmendoza M, Velascoarroyo B, Gonzálezmelendi P, Martínez M, Díaz I. 2014.** C1A
505 cysteine protease-cystatin interactions in leaf senescence. *Journal of Experimental*

- 506 *Botany* **65(14)**:3825-33 DOI 10.1093/jxb/eru043.
- 507 **Dugas DV, Monaco MK, Olson A, Klein RR, Kumari S, Ware D, Klein PE. 2011.** Functional
508 annotation of the transcriptome of *Sorghum bicolor* in response to osmotic stress and
509 abscisic acid. *BMC Genomics* **12**:514 DOI 10.1186/1471-2164-12-514.
- 510 **Dutt S, Singh VK, Marla SS, Kumar A. 2010.** In silico analysis of sequential, structural and
511 functional diversity of wheat cystatins and its implication in plant defense. *Genomics*
512 *Proteomics Bioinformatics* **8(1)**:42-56 DOI 10.1016/S1672-0229(10)60005-8.
- 513 **Finn RD, Clements J, Eddy SR. 2011.** HMMER web server: interactive sequence similarity
514 searching. *Nucleic Acids Research* **39**:29-37 DOI 10.1093/nar/gkr367.
- 515 **Gaddour K, Carbajosa JV, Lara P, Almoneda PI, Diaz I, Carbonero P. 2001.** A constitutive
516 cystatin-encoding gene from barley (Icy) responds differentially to abiotic stimuli. *Plant*
517 *Molecular Biology* **45**:599-608 DOI 10.1023/a:1010697204686.
- 518 **Goulet MC, Dallaire C, Vaillancourt LP, Khalf M, Badri AM, Preradov A, Duceppe MO,**
519 **Cloutier GC, Michaud CD. 2008.** Tailoring the specificity of a plant cystatin toward
520 herbivorous insect digestive cysteine proteases by single mutations at positively selected
521 amino acid sites. *Plant Physiology* **146**:1010-1019 DOI 10.2307/40065908.
- 522 **Gu Z, Cavalcanti A, Chen FC, Bouman P, Li WH. 2002.** Extent of gene duplication in the
523 genomes of *Drosophila*, nematode, and yeast. *Molecular Biology Evolution* **19(3)**:256-
524 262 DOI 10.1093/oxfordjournals.molbev.a004079.
- 525 **Hashimoto S, Tezuka T, Yokoi S. 2019.** Morphological changes during juvenile-to-adult phase
526 transition in Sorghum. *Planta* **250**:1557-1566 DOI 10.1007/s00425-013-1895-z.
- 527 **Hu B, Jin J, Guo AY, Zhang H, Luo J, Gao G. 2014.** GSDS 2.0: an upgraded gene feature
528 visualization server. *Bioinformatics* **31(8)**:1296 DOI 10.1093/bioinformatics/btu817.

- 529 **Hu YJ, Irene D, Lo CJ, Cai YL, Tzen TC, Lin TH, Chyan CL. 2015.** Resonance assignments
530 and secondary structure of a phytocystatin from *Sesamum indicum*. *Biomolecular NMR*
531 *Assignments* **9**:309-311 DOI 10.1007/s12104-015-9598-y.
- 532 **Huang Y, Xiao B, Xiong L. 2007.** Characterization of a stress responsive proteinase inhibitor
533 gene with positive effect in improving drought resistance in rice. *Planta* **226**:73-85 DOI
534 10.2307/23389651.
- 535 **Hwang JE, Hong JK, Lim CJ, Chen H, Je J, Yang KA, Kim DY, Choi YJ, Lee SY, Lim CO.**
536 **2010.** Distinct expression patterns of two *Arabidopsis* phytocystatin genes, AtCYS1 and
537 AtCYS2, during development and abiotic stresses. *Plant Cell Reports* **29**:905-915 DOI
538 10.1007/s00299-010-0876-y.
- 539 **Jenko S, Dolenc I, Guncar G, Dobersek A, Podobnik M, Turk D. 2003.** Crystal structure of
540 Stefin A in complex with cathepsin H: N-terminal residues of inhibitors can adapt to the
541 active sites of endo- and exopeptidases. *Journal Molecular Biology* **326(3)**:875-885 DOI
542 10.1016/s0022-2836(02)01432-8.
- 543 **Kebrom TH, Brutnell TP, Finlayson SA. 2010.** Suppression of sorghum axillary bud
544 outgrowth by shade, phyB and defoliation signalling pathways. *Plant Cell Environment*
545 **33(1)**:48-58 DOI 10.4161/psb.5.3.11186.
- 546 **Kiggundu A, Muchwezi J, Van C, Viljoen A, Vorster J, Schlüter U, Kunert K, Michaud D.**
547 **2010.** Deleterious effects of plant cystatins against the banana weevil *Cosmopolites*
548 *sordidus*. *Arch Insect Biochemistry Physiology* **73(2)**:87-105 DOI 10.1002/arch.20342.
- 549 **Kiyosaki T, Matsumoto I, Asakura T, Funaki J, Kuroda M, Misaka T, Arai S, Abe K. 2007.**
550 Gliadain, a gibberellin-inducible cysteine proteinase occurring in germinating seeds of
551 wheat, *Triticum aestivum* L., specifically digests gliadin and is regulated by intrinsic

- 552 cystatins. *FEBS Journal* **164**:470-477 DOI 10.1111/j.1742-4658.2007.05749.x.
- 553 **Krzywinski M, Schein J, Birol I, Connors J, Gascoyne R, Horsman D, Jones SJ, Marra MA.**
554 **2009.** Circos: an information aesthetic for comparative genomics. *Genome research*
555 **19(9)**:1639-1645 DOI 10.1101/gr.092759.109.
- 556 **Li J, Yang XW, Li YC, Niu JS, He DX. 2017.** Proteomic analysis of developing wheat grains
557 infected by powdery mildew (*Blumeria graminis* f.sp. *tritici*). *Journal of Plant*
558 *Physiology* **215**:140-153 DOI 10.1016/j.jplph.2017.06.003.
- 559 **Li SF, Su T, Cheng GQ, Wang BX, Li X, Deng CL, Gao WJ. 2017.** Chromosome evolution in
560 connection with repetitive sequences and epigenetics in plants. *Genes* **8**:290 DOI
561 10.3390/genes8100290.
- 562 **Lima AM, dos Reis SP, de Souza CR. 2015.** Phytocystatins and their potential to control plant
563 diseases caused by fungi. *Protein and Peptid Letters* **22**:104-111 DOI
564 10.2174/0929866521666140418101711.
- 565 **Lozano R, Hamblin MT, Prochnik S, Jannink JL. 2015.** Identification and distribution of the
566 NBS-LRR gene family in the Cassava genome. *BMC Genomics* **16(1)**:360 DOI
567 10.1186/s12864-015-1554-9.
- 568 **Margis R, Reis EM, Villeret V. 1998.** Structural and phylogenetic relationships among plant
569 and animal cystatins. *Arch Biochemistry Biophysics* **359(1)**:24-30 DOI
570 10.1006/abbi.1998.0875.
- 571 **Martinez M, Abraham Z, Gambardella M, Echaide M, Carbonero P, Diaz I. 2005.** The
572 strawberry gene *Cyfl* encodes a phytocystatins with antifungal activity. *Journal of*
573 *Experimental Botany* **56**:1821-1829 DOI 10.1093/jxb/eri172.
- 574 **Martinez M, Cambra I, Carrillo L, Diazmendoza M, Diaz I. 2009.** Characterization of the

- 575 entire cystatin gene family in barley and their target cathepsin L-like cysteine-proteases,
576 partners in the hordein mobilization during seed germination. *Plant Physiology*
577 **151(3):1531-1545** DOI 10.1104/pp.109.146019.
- 578 **Martinez M, Diazmendoza M, Carrillo L, Diaz I. 2007.** Carboxy terminal extended
579 phytocystatins are bifunctional inhibitors of papain and legumain cysteine proteinases.
580 *FEBS Letters* **581(16):2914-2918** DOI 10.1016/j.febslet.2007.05.042.
- 581 **Martinez M, Diaz I. 2008.** The origin and evolution of plant cystatins and their target cysteine
582 proteinases indicate a complex functional relationship. *BMC Evolutionary Biology*
583 **8(1):198-210** DOI 10.1186/1471-2148-8-198.
- 584 **Martinez M, Santamaria ME, Diazmendoza M, Arnaiz A, Carrillo L, Ortego F, Diaz I.**
585 **2016.** Phytocystatins: defense proteins against phytophagous insects and acari.
586 *International Journal of Molecular Sciences* **17(10):1747-1763** DOI
587 10.3390/ijms17101747.
- 588 **Massonneau A, Condamine P, Wisniewski J P, Zivy M, Rogowsky PM. 2005.** Maize
589 cystatins respond to developmental cues, cold stress and drought. *Biochimica et Biophysica*
590 *Acta* **1729:186-199** DOI 10.1016/j.bbaexp.2005.05.004.
- 591 **Melo FR, Mello MO, Franco OL, Rigden DJ, Mello LV, Genú AM, Silvafilho MC, Gleddie**
592 **S, Grossidesá MF. 2003.** Use of phage display to select novel cystatins specific for
593 *Acanthoscelides obtectus* cysteine proteinases. *BBA-Proteins Proteomics* **1651(1):146-**
594 **152** DOI 10.1016/S1570-9639(03)00264-4.
- 595 **Meriem B, Urte S, Juan V, Marie-Claire G, Dominique M. 2010.** Plant cystatins. *Biochimie*
596 **92(11):1657-1666** DOI 10.1016/j.biochi.2010.06.006.
- 597 **Nagata K, Kudo N, Abe K, Arai S, Tanokura M. 2000.** Three-dimensional solution structure

- 598 of oryzacystatin-I, a cysteine proteinase inhibitor of the rice, *Oryza sativa* L. japonica.
599 *Biochemistry* **39**:14753-14760 DOI 10.1021/bi0006971.
- 600 **Paterson AH, Bowers JE, Bruggmann R, Dubchak I, Grimwood J, Gundlach H, Haberer G,**
601 **Hellsten U, Mitros T, Poliakov A. 2009.** The *Sorghum bicolor* genome and the
602 diversification of grasses. *Nature* **457(7229)**:551-556 DOI 10.1038/nature07723.
- 603 **Peitsch M. 1996.** ProMod and Swiss-Model: internet-based tools for automated comparative
604 protein modeling. *Biochemical Society Transactions* **224**:274-279 DOI
605 10.1042/bst0240274.
- 606 **Pfaffl MW. 2001.** A new mathematical model for relative quantification in real-time RT-PCR.
607 *Nucleic Acids Research* **29**:e45 DOI 10.1093/nar/29.9.e45.
- 608 **Pirovani CP, Santiago AS, Santos LS, Micheli F, Margis R, Silva Gesteira R, Alvim FC,**
609 **Pereira GAG, Mattos JC. 2010.** *Theobroma cacao* cystatins impair *Moniliophthora*
610 *perniciosa* mycelial growth and are involved in postponing cell death symptoms. *Planta*
611 **232(6)**:1485-1497 DOI 10.2307/23391912.
- 612 **Sayle R, Milner-White EJ. 1995.** RasMol: biomolecular graphics for all. *Trends in Biochemical*
613 *Sciences* **20**:374 DOI 10.1016/S0968-0004(00)89080-5.
- 614 **Song C, Kim T, Chung WS, Lim CO. 2017.** The *Arabidopsis* phytocystatin AtCYS5 enhances
615 seed germination and seedling growth under heat stress conditions. *Molecular Cells*
616 **40(8)**:577-586 DOI 10.14348/molcells.2017.0075.
- 617 **Strömvik MV, Fauteux F. 2009.** Seed storage protein gene promoters contain conserved DNA
618 motifs in *Brassicaceae*, *Fabaceae* and *Poaceae*. *BMC Plant Biology* **9**:126 DOI
619 10.1186/1471-2229-9-126.
- 620 **Stubbs MT, Laber B, Bode W, Huber R, Jerala R, Lenarcic B, Turk V. 1990.** The refined

- 621 2.4 A X-ray crystal structure of recombinant human stefin B in complex with the cysteine
622 proteinase papain: a novel type of proteinase inhibitor interaction. *Embo Journal*
623 **9(6)**:1939-1947 DOI 10.1002/j.1460-2075.1990.tb08321.x.
- 624 **Subburaj S, Zhu D, Li X, Hu Y, Yan Y. 2017.** Molecular characterization and expression
625 profiling of *Brachypodium distachyon* L. cystatin genes reveal high evolutionary
626 conservation and functional divergence in response to abiotic stress. *Frontiers in Plant*
627 *Science* **8**:743 DOI 10.3389/fpls.2017.00743.
- 628 **Sunita K, Klein RR, Andrew O, Monaco MK, Dugas DV, Doreen W, Klein PE. 2011.**
629 Functional annotation of the transcriptome of *Sorghum bicolor* in response to osmotic
630 stress and abscisic acid. *BMC Genomics* **12(1)**:514-514 DOI 10.1186/1471-2164-12-514.
- 631 **Tan Y, Yang Y, Li C, Liang B, Li M, Ma F. 2017.** Overexpression of *MpCYS4*, a phytocystatin
632 gene from *Malus prunifolia* (Willd.) Borkh., delays natural and stress-induced leaf
633 senescence in apple. *Plant Physiology Biochemistry* **115**:219-28 DOI
634 10.1016/j.plaphy.2017.03.025.
- 635 **Taylor SH, Hulme SP, Rees M, Ripley BS, Woodward FI, Osborne CP. 2010.**
636 Ecophysiological traits in C₃ and C₄ grasses: A phylogenetically controlled screening
637 experiment. *New Phytologist* **185(3)**:780-791 DOI 10.1111/j.1469-8137.2009.03102.x.
- 638 **Tetreault HM, Grover S, Scully ED, Gries T, Palmer N, Sarath G, Louis J, Sattler SE. 2019.**
639 Global responses of resistant and susceptible Sorghum (*Sorghum bicolor*) to sugarcane
640 aphid (*Melanaphis sacchari*). *Frontiers in Plant Science* **10**:145 DOI
641 10.3389/fpls.2019.00145.
- 642 **Valdes-Rodriguez S, Galvan-Ramirez JP, Guerrero-Rangel A, Cedro-Tanda A. 2015.**
643 Multifunctional amaranth cystatin inhibits endogenous and digestive insect cysteine

- 644 endopeptidases: A potential tool to prevent proteolysis and for the control of insect pests.
645 *Biotechnology Applied Biochemistry* **62**:634-641 DOI 10.1002/bab.1313.
- 646 **Velasco-Arroyo B, Diaz-Mendoza M, Gomez-Sanchez A, Moreno-Garcia B, Santamaria**
647 **ME, Torija-Bonilla M, Hensel G, Kumlehn J, Martinez M, Diaz I 2018.** Silencing
648 barley cystatins HvCPI-2 and HvCPI-4 specifically modifies leaf responses to drought
649 stress. *Plant Cell and Environment* **41(8)**:1776-1790 DOI 10.1111/pce.13178.
- 650 **Wang B, Regulsk M, Tseng E, Olson A, Goodwin S, McCombie WR, Ware D. 2018.** A
651 comparative transcriptional landscape of maize and Sorghum obtained by single-
652 molecule sequencing. *Genome Research* **28(6)**:921-928 DOI 10.1101/gr.227462.117.
- 653 **Wang HW, Hwang SG, Karuppanapandian T, Liu AH, Kim W, Jang CS. 2012.** Insight into
654 the molecular evolution of non-specific lipid transfer proteins via comparative analysis
655 between rice and sorghum. *DNA Research* **19**:179-194 DOI 10.1093/dnares/dss003.
- 656 **Wang W, Zhao P, Zhou XM, Xiong HX, Sun MX. 2015.** Genome-wide identification and
657 characterization of cystatin family genes in rice (*Oryza sativa* L.). *Plant Cell Reports*
658 **34(9)**:1579-1592 DOI 10.1007/s00299-015-1810-0.
- 659 **Wen G. 2017.** A simple process of RNA-Sequence analyses by Hisat2, Htseq and DESeq2.
660 *International Conference* **Pp**:11-15 DOI 10.1145/3143344.3143354.
- 661 **Xu G, Guo C, Shan H, Kong H. 2012.** Divergence of duplicate genes in exon-intron structure.
662 *PNAS* **109(4)**:1187-1192 DOI 10.1073/pnas.1109047109.
- 663 **Yadav CB, Bonthala VS, Muthamilarasan M, Pandey G, Khan Y, Prasad M. 2015.**
664 Genome-wide development of transposable elements-based markers in foxtail millet and
665 construction of an integrated database. *DNA Research* **22**:79-90 DOI
666 10.1093/dnares/dsu039.

- 667 **Yan S, Li SJ, Zhai GW, Lu P, Deng H, Zhu S, Huang RL, Shao JF, Tao YZ, Zou GH. 2017.**
668 Molecular cloning and expression analysis of duplicated polyphenol oxidase genes reveal
669 their functional differentiations in Sorghum. *Plant Science* **263**:23-30 DOI
670 10.1016/j.plantsci.2017.07.002.
- 671 **Yazawa T, Kawahigashi H, Matsumoto T, Mizuno H. 2013.** Simultaneous transcriptome
672 analysis of Sorghum and *Bipolaris sorghicola* by using RNA-seq in combination with *De*
673 *novo* transcriptome assembly. *PLoS One* **8(4)**:e62460 DOI
674 10.1371/journal.pone.0062460.
- 675 **Yuan S, Li R, Wang L, Chen H, Zhang C, Chen L, Hao Q, Shan Z, Zhang X, Chen S. 2016.**
676 Search for nodulation and nodule development-related cystatin genes in the genome of
677 soybean (*Glycine max*). *Frontiers in Plant Science* **7**:1595 DOI 10.3389/fpls.2016.01595.
- 678 **Zhang X, Liu S, Takano T. 2008.** Two cysteine proteinase inhibitors from *Arabidopsis thaliana*,
679 AtCYSa and AtCYSb, increasing the salt, drought, oxidation and cold tolerance. *Plant*
680 *Molecular Biology* **68**:131-143 DOI 10.1007/s11103-008-9357-x.
- 681 **Zhao P, Zhou XM, Zou J, Wang W, Wang L, Peng XB, Sun MX. 2014.** Comprehensive
682 analysis of cystatin family genes suggests their putative functions in sexual reproduction,
683 embryogenesis, and seed formation. *Journal of Experimental Botany* **65(17)**:5093-5108
684 DOI 10.1093/jxb/eru274.
- 685 **Zhang Z, Li J, Zhao XQ, Wang J, Wong GK, Yu J. 2006.** KaKs_Calculator 2.0: Calculating
686 Ka and Ks through model selection and model averaging. *Genomics Proteomics*
687 *Bioinformatics* **4(4)**:259-263 DOI 10.1016/S1672-0229(10)60008-3.
- 688
- 689

690

691

Figure 1

Chromosome localization of *SbCys* genes.

Chromosome number is indicated at the top of each bar. The size of chromosome was labeled on the left of the figure.

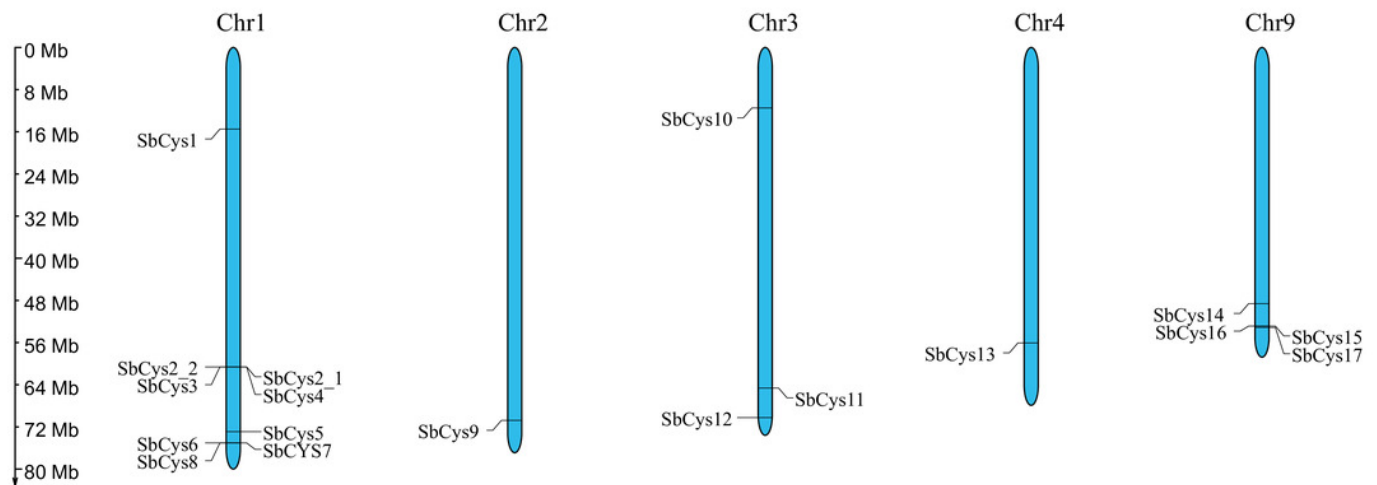


Figure 2

Phylogenetic relationship and gene structure of *SbCys* genes.

A phylogenetic tree was constructed using MEGA X by the maximum likelihood method with 1000 bootstrap replicates. Exon/intron structures were identified by online tool GSDS.

Lengths of exons and introns of each *SbCys* genes were exhibited proportionally. Exons and introns are shown by blue bars and black horizontal lines, respectively.

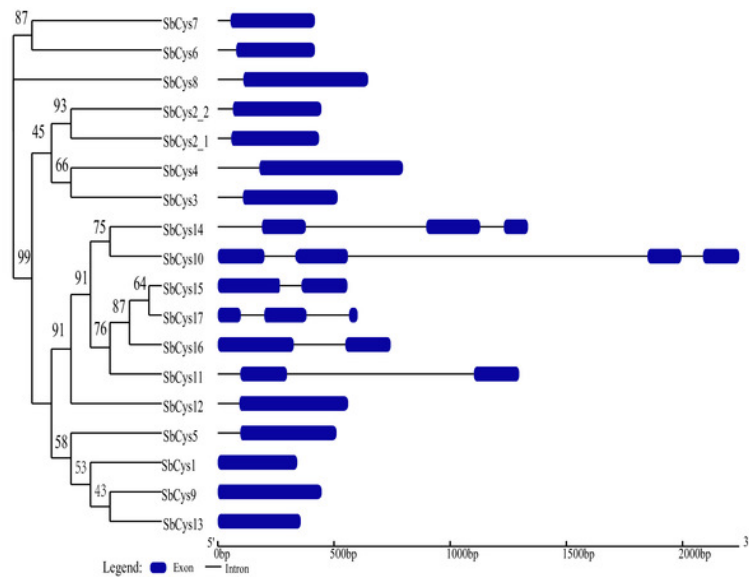


Figure 4

The three-dimensional structure prediction of Sorghum cystatins.

(A) The three-dimensional structures of SbCys proteins were predicted using the automated SWISS-MODEL program with OC-I as a template. (B) The three-dimensional structure of SbCys10 was predicted using the automated SWISS-MODEL program with SiCYS as a template. Two important motifs involved in the interaction with the target enzymes are indicated: the reactive site (asterisks) and W residue (crosses).

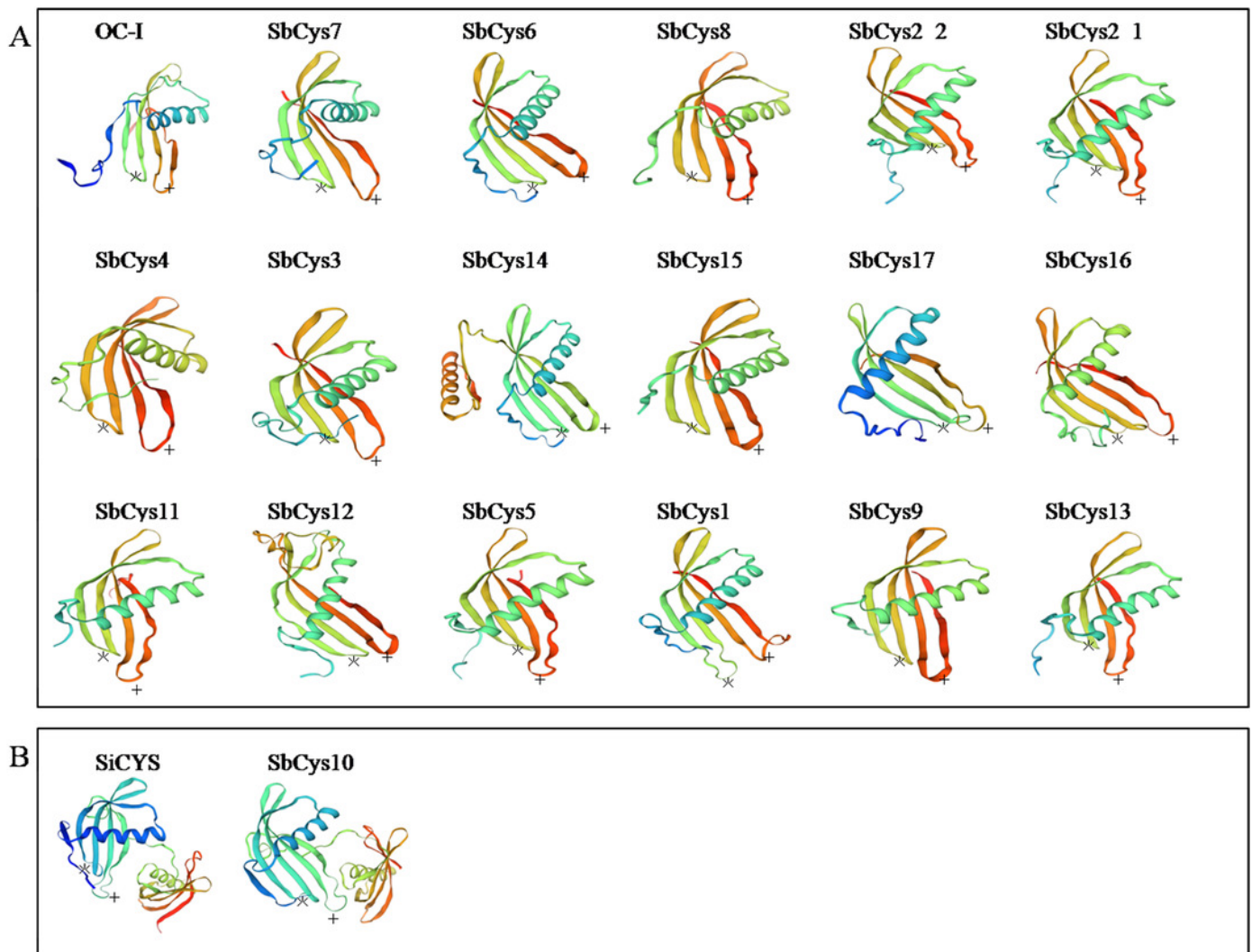


Figure 5

Phylogenetic relationships of the cystatins from *Arabidopsis*, rice, barley and Sorghum.

The phylogenetic tree was constructed by MEGA X with the maximum likelihood method. The numbers at the nodes indicate the bootstrap values. Gene names with black, red, and blue represented Group I, Group II, and Group III, respectively.

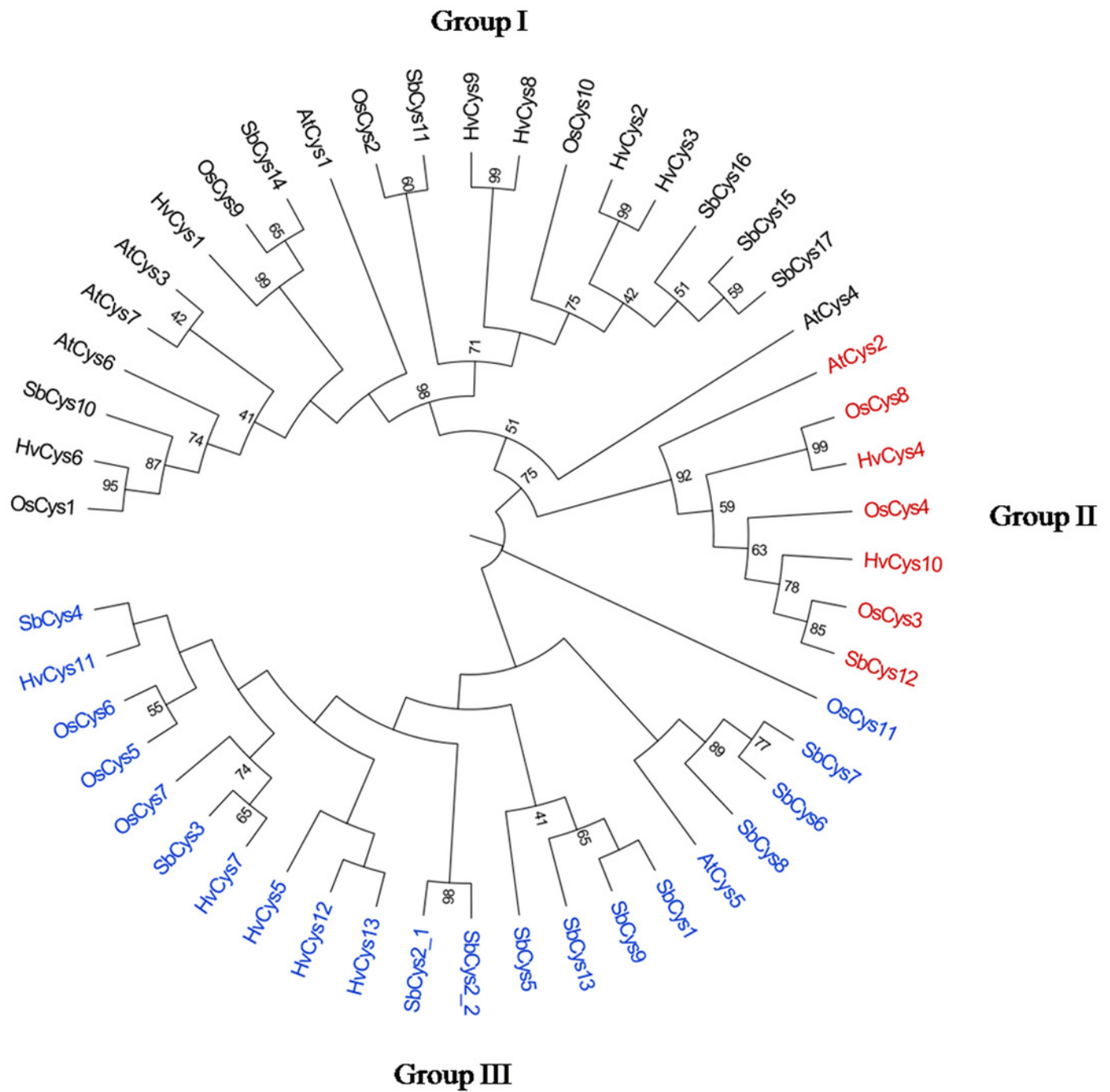


Figure 6

The distribution of *cis*-elements in the 1.5 kb upstream promoter regions of *SbCys* genes.

The *cis*-elements in the promoter region of *SbCys* genes were predicted using PlantCARE database (<http://bioinformatics.psb.ugent.be/webtools/plantcare/html/>). Different *cis*-elements were represented by different shapes and colors.

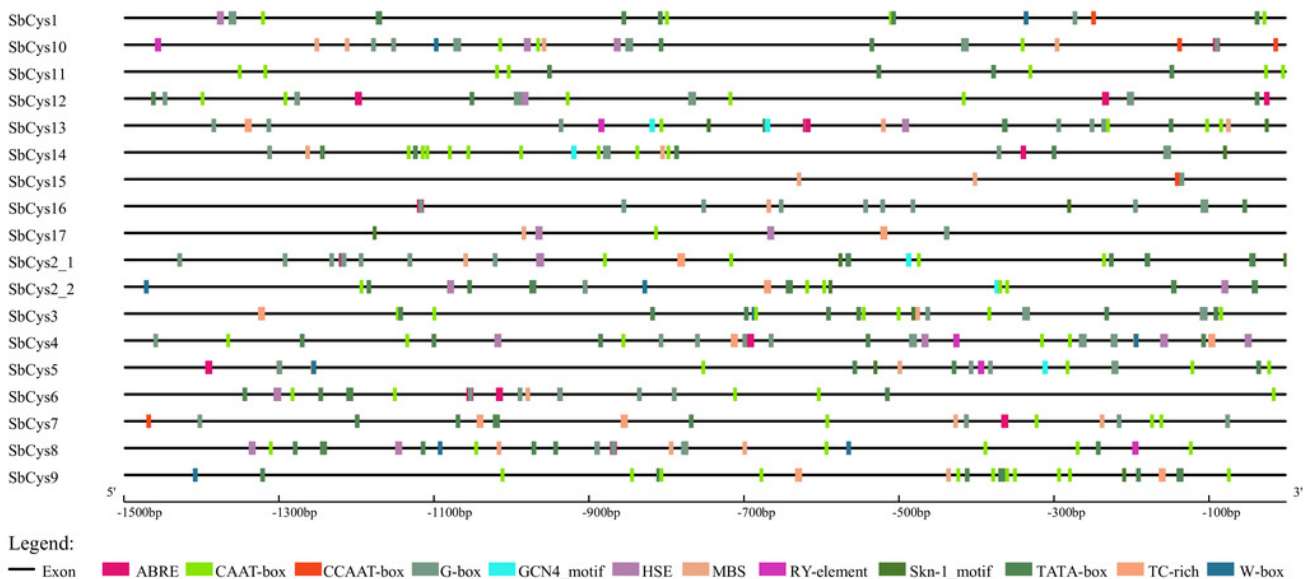


Figure 7

The interaction networks of SbCys proteins according to the orthologs in *Arabidopsis*.

Functional interacting network models were integrated using the STRING tool, and the confidence parameters were set at a 0.40 threshold. Homologous genes in Sorghum and *Arabidopsis* are shown in black and red, respectively.

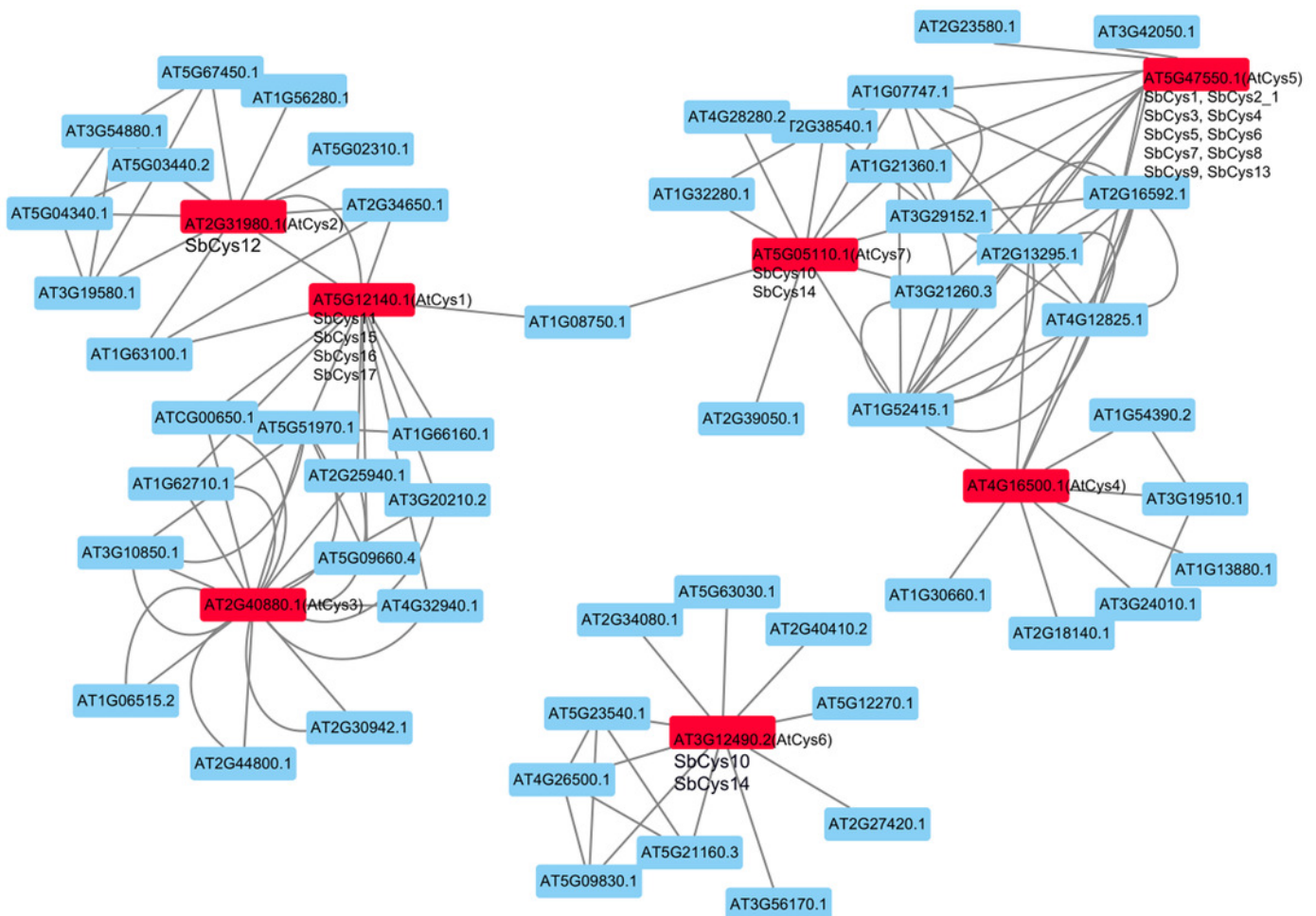


Figure 8

Hierarchical clustering of the expression profiles of *SbCys* genes in different tissues .

Different tissues are exhibited below each column. Root, shoot, and whole organism belonged to vegetable tissues were collected at 14 days after Sorghum seed germination. Reproductive tissues included embryo , endosperm and pericarp were collected at 20 days after pollination; pollens at booting stage; Inflorescences based on sizes: 1-5 mm, 5-10 mm, and 1-2 cm. Log transform data was used to create the heatmap. The scale bar represented the fold change (color figure online). Blue blocks represented the lower expression level and red blocks represented the higher expression level.

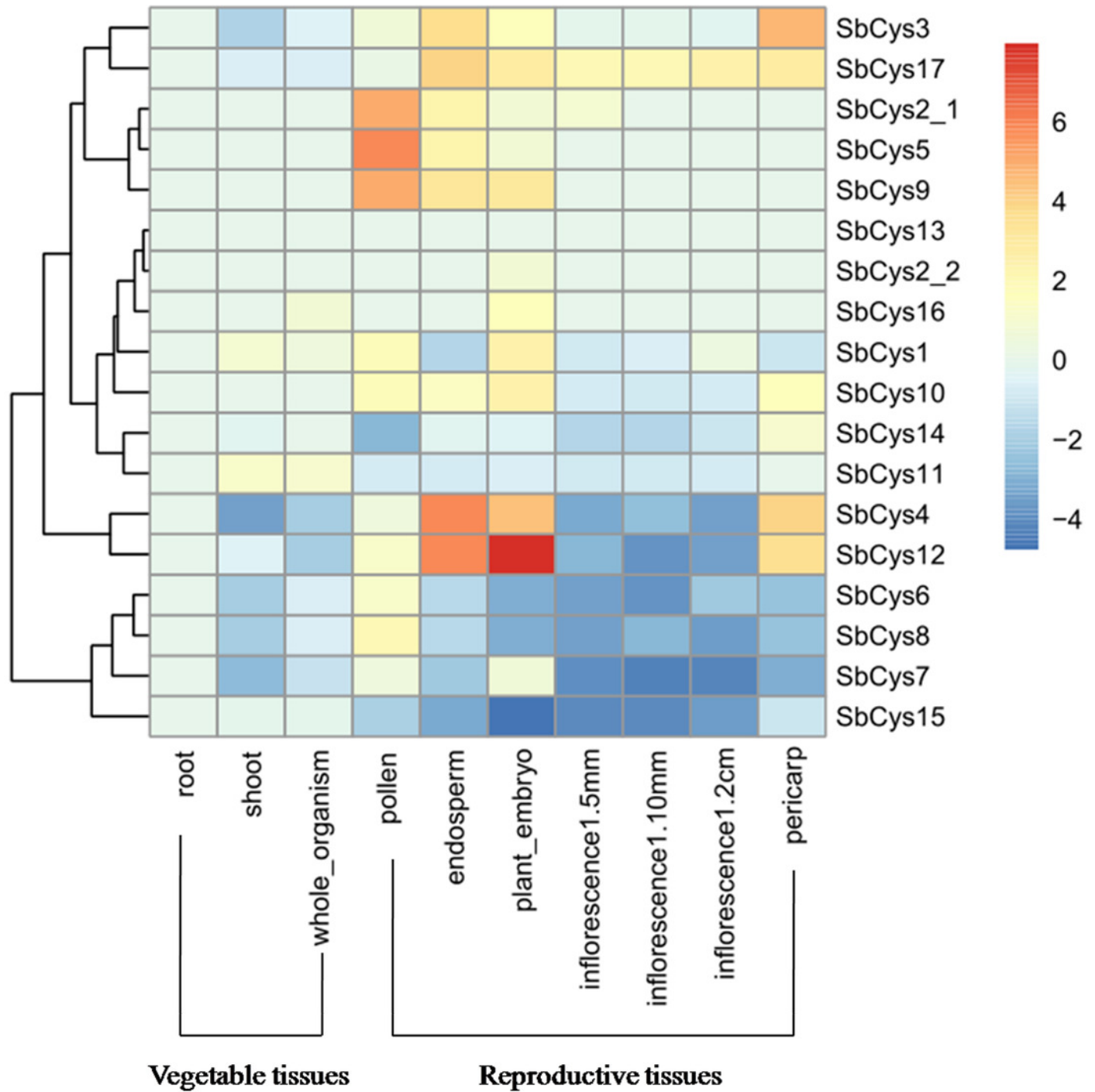


Figure 9

Hierarchical clustering of the expression profiles of *SbCys* genes under biotic stresses.

(A) The expression changes in *SbCys* genes at 0, 12, and 24 hours with *Bipolaris sorghicola* infection. (B) The expression changes of *SbCys* genes at 5, 10, 15 days with sugarcane aphid infestation. Log transform data was used to create the heatmap. The scale bar represents the fold change (color figure online). Blue blocks indicate low expression and red blocks indicate high expression (color figure online).

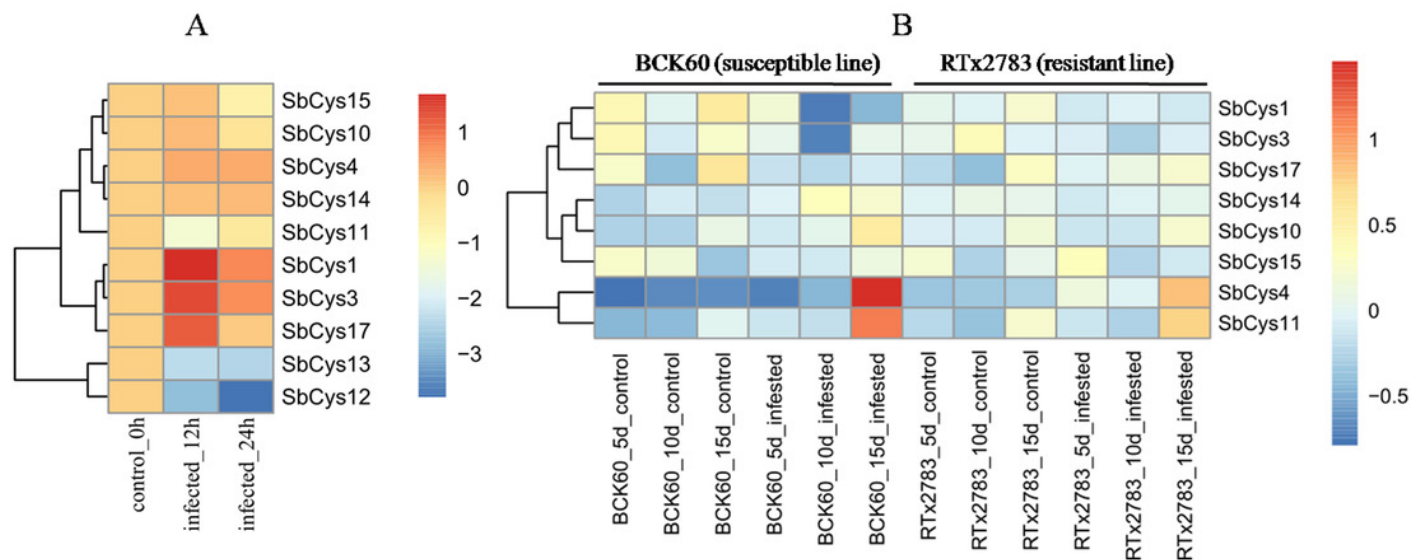


Figure 10

Expression profiles of *SbCys* genes at 5, 10, and 15 days with sugarcane aphid infection.

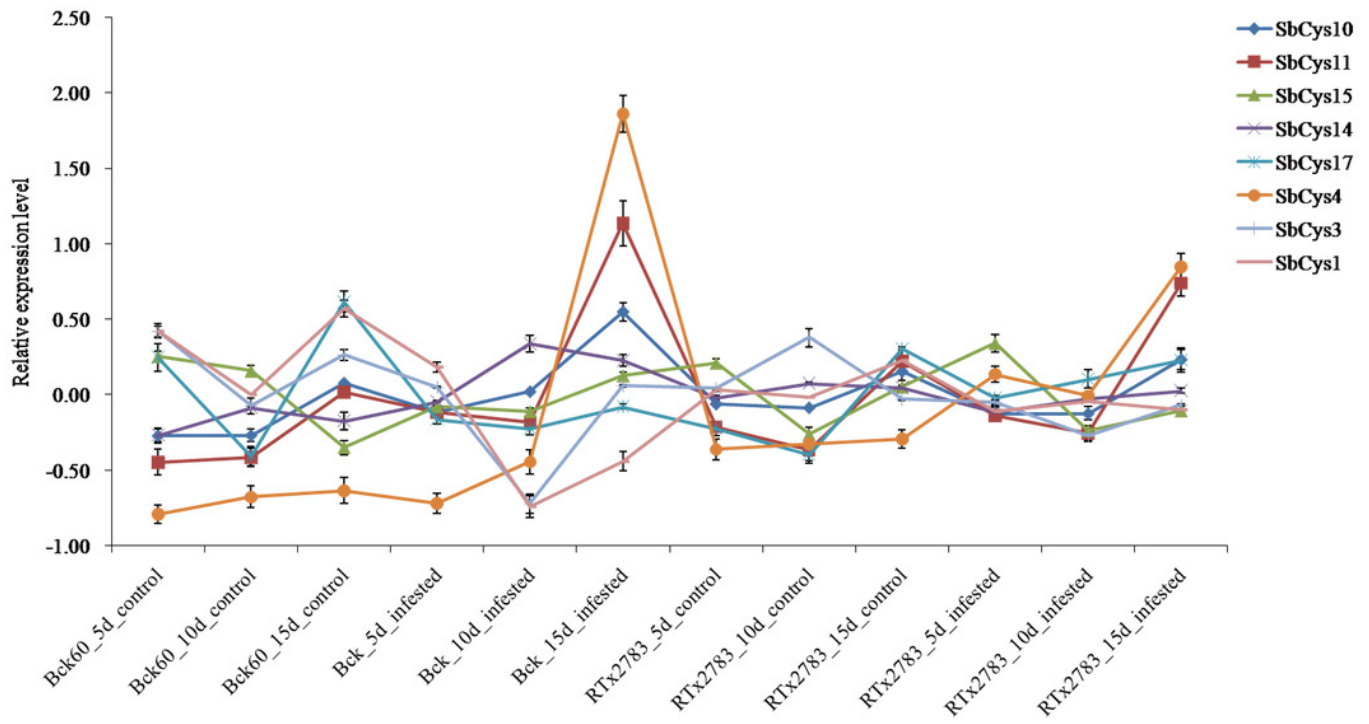


Figure 11

Expression patterns of *SbCys* genes under (A) dehydration (PEG 6,000) treatment, (B) salt shock (NaCl) treatment, and (C) ABA treatment.

qRT-PCR was used to investigate the expression levels of each *SbCys* gene. To visualize the relative expression levels data, 0 h at each treatment was normalized as "1". * indicated significant differences in comparison with the control at $p \leq 0.05$. ** indicated significant differences in comparison with the control at $p \leq 0.01$.

